第 43 卷 第 23 期/2023 年 12 月/光学学报 研究论文

光学学报

基于电流内调制DFB激光器的高空间分辨率OFDR

张嘉彤，苏丽文，刘畅，楚妍妍，付兴虎，金娃，毕卫红，付广伟*

燕山大学信息科学与工程学院河北省特种光纤与光纤传感重点实验室，河北 秦皇岛 066004

摘要 针对光频域反射(OFDR)系统中光源调频非线性导致的传感单元定位误差、传感精度低、传感范围窄、系统适应性差等问题，提出了开环校正结合光电锁相环闭环校正电流内调制分布反馈式半导体(DFB)激光器的方法。该方法用于控制DFB激光器连续、快速、大范围频率扫描线性化，使其成为OFDR系统的优质光源，提高OFDR的分辨率。实验结果表明DFB激光器的扫频非线性度由16.55%下降至0.078%，拍频信号中心频率的功率提升了21.1 dB，探测范围由15 m提升至50 m，测量值与实际值的最大误差为3.79 mm，重复性测量的最大标准偏差为112.2 μm。

关键词 激光器；分布反馈式半导体激光器；光频域反射；频率扫描线性化；光电锁相环

中图分类号 TN212 **文献标志码** A **DOI**：10.3788/AOS231034

1 引 言

光频域反射(OFDR)技术[1]是一种基于光学干涉原理的高分辨率光学传感技术。OFDR技术可以实现对光纤等光学传感器件的高精度、高分辨率的非接触式测量和监测[2]。

传统的分布式光纤传感技术主要采用光时域反射(OTDR)技术[3]，该技术通过向光纤注入脉冲光信号，利用脉冲光信号在光纤中的传输、反射、散射等特性，实现对光纤中故障点的定位和距离的测量以及对待测点传感参量的测量[4-6]。然而，由于电子瓶颈的存在，OTDR技术在分辨率、灵敏度和探测深度等方面存在一定的局限性[7]，难以满足高精度、高分辨率、大范围的光学传感需求[8]。OFDR技术则采用了一种全新的测量原理，即将激光信号以频率扫描的形式注入到光纤中，通过检测激光信号在光纤中反射和散射后的干涉信号，实现对光纤中故障点的定位和距离的测量[9]。OFDR系统不仅具有高精度、高分辨率和大范围的特点，还具有实时性强、信噪比高等优点。2015年，刘琨等[10]提出基于OFDR技术的光纤连续分布式定位应变测量传感方法，实现了100 m范围内光纤应变大小及分布位置的传感，系统空间分辨率为20 cm。2021年，Xu等[11]利用飞秒激光逐点法在单模光线中制备全同弱反射光栅阵列，实现了传感长度为2 m、分辨率为10 mm、温度测量范围为1000 ℃的分布式高温传感。因此，OFDR技术在航空[11-12]、交通[13-14]、通信[15]等领域中具有广泛的应用前景。OFDR已经过几十年的发展，目前限制该技术进一步发展的瓶颈在于扫频光源难以实现和信号处理较难优化。

光源是OFDR系统中至关重要的组成部分，光源的调频线性度直接影响了系统的性能、精度和分辨率，目前系统通常采用的光源是机械调谐的二极管激光器[16]，虽然其拥有调频范围广、线宽窄等特点，但是其成本难以降低，使用寿命难以延长。电流直接调制的分布反馈式半导体(DFB)激光器[17]以其成本低、调频方式简便等优势，成为OFDR系统的潜在的优质光源，但是其存在的相位噪声与调频线性度差的问题亟待解决。

本文提出了开环校正结合光电锁相环闭环校正DFB激光器的方法，采用电流直接调制的DFB激光器，基于自外差马赫-曾德尔干涉仪(MZI)产生的拍频信号量化DFB激光器的调谐特性，采用开环校正对激光器的驱动信号进行预校正，光电锁相环由鉴频鉴相器、自适应环路滤波器和任意信号发生器构成，将实际拍频信号与理想拍频信号的相位误差反馈至驱动信号，实现对DFB激光器调频的闭环校正。分析不同校正阶段的DFB激光器的调频特性，并利用校正后的系统对不同长度的光纤进行测量，在50 m范围内，测量

收稿日期：2023-05-24；**修回日期**：2023-08-04；**录用日期**：2023-09-04；**网络首发日期**：2023-09-14

基金项目：国家自然科学基金(61575170)、河北省自然科学基金(F2021203045，F2021203058)、河北省科技支撑计划(216Z1702G，216Z1706G)

通信作者：*earl@ysu.edu.cn

值与实际值的最大误差为3.79 mm，系统的重复性测量的最大标准偏差为112.2 μm。

2　基本原理

2.1　OFDR基本原理

OFDR的概念最早由德国科学家Eickhoff等在1981年提出，依据线性调频连续波雷达的调频连续波（FMCW）技术，其基本原理如图1所示。本文所采用的电流调谐DFB激光器作用的OFDR传感系统中，激光器产生的调频光经耦合器1分为两束光，两束光分别进入自外差MZI的参考臂与探测臂：进入参考臂的调频光直接进入耦合器2；进入探测臂的调频光通过环形器进入待测光纤（FUT）并在其端面发生瑞利散射，之后经环形器进入耦合器2。两束调频光在耦合器2处发生干涉并产生拍频信号，光电探测器对拍频信号进行检测与处理。拍频信号的频率反映了待测点的位置信息，若待测光纤中存在不同的探测点，则会产生不同频率的拍频信号，在信号处理部分采用窗函数等方式处理拍频信号的傅里叶变换（FFT）结果，对不同频率的拍频信号进行分离，即可得到不同探测点的拍频信号的幅度与频率信息。

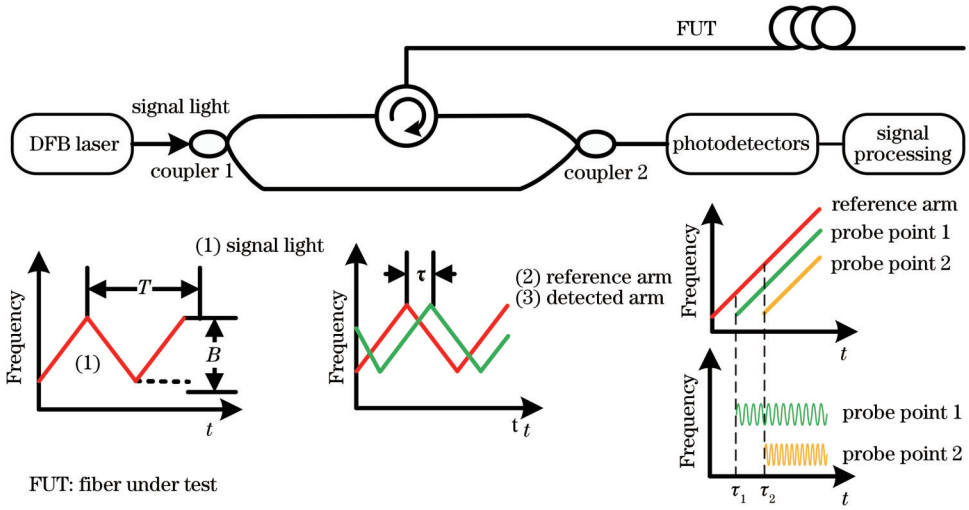

图1　OFDR原理图

Fig. 1　Schematic diagram of OFDR

激光器产生的发射信号到达耦合器2的强度$I_t(t)$以及待测点散射产生的回波信号到达耦合器2的强度$I_r(t)$可以分别表示为

$$I_t(t)=u_t\sin(\omega_t t+\theta_t),\tag{1}$$

$$I_r(t)=u_r\sin[\omega_t(t-\tau)+\theta_r],\tag{2}$$

式中：u_t、u_r分别为发射信号和回波信号的强度峰值；ω_t为发射信号的角频率；θ_t、θ_r分别为发射信号和回波信号的初始相位；τ为两束光到达耦合器2的时间差。

调频信号的调频速率可以表示为

$$k=\frac{2B}{T},\tag{3}$$

式中：B为调频范围；T为调频周期。

发射信号与回波信号在光电探测器处发生干涉后的信号可以表示为

$$I(t)=u[I_t(t)+I_r(t)]^2,\tag{4}$$

式中：u为光电探测器的增益系数。

光电探测器的输出电信号可以表示为

$$I_o(t)=2u_t u_r u[\cos(\omega_t-\omega_r)t+(\theta_t-\theta_r)]。\tag{5}$$

拍频信号的频率可以表示为

$$f_{beat}=\frac{1}{2\pi}(\omega_t-\omega_r)=\frac{1}{2\pi}k\tau=\frac{2B\tau}{T\pi}。\tag{6}$$

最终，通过拍频信号的频率信息，即可反推探测点位置，并可以通过拍频信号的幅度变化量或频率偏移量反演探测点的传感信息。

2.2　开环校正模型

在OFDR系统中，DFB激光器的发射调频光的瞬时频率可以表示为

$$f_{out}=f_o+i(t)K[i(t)],\tag{7}$$

式中：$i(t)$为激光器的驱动电流；K为激光器发射激光频率随电流变化的调频速率；f_o为激光器发射激光的初始频率。

系统达到线性调频的条件为

$$f_{beat}=k\tau=\tau\frac{\mathrm{d}f_{out}}{\mathrm{d}t}。\tag{8}$$

将式(7)代入式(8)后可得到

$$f_{beat}=\tau\frac{\mathrm{d}\{f_o+i(t)K[i(t)]\}}{\mathrm{d}t}=\frac{\mathrm{d}i(t)}{\mathrm{d}t}\left\{\tau\frac{\mathrm{d}K[i(t)]}{\mathrm{d}t}i(t)+\tau K[i(t)]\right\}=\frac{\mathrm{d}i(t)}{\mathrm{d}t}H[i(t)]。\tag{9}$$

DFB激光器开环校正过程如图2所示，采用固定

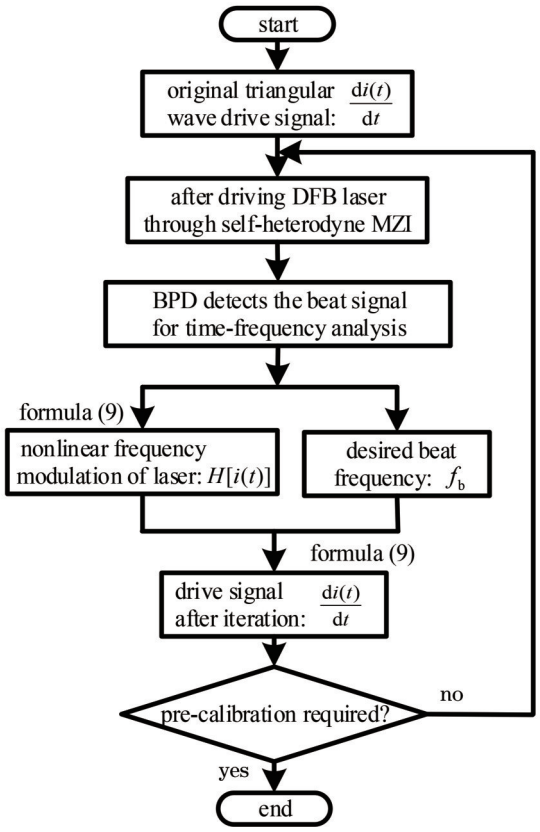

图 2　DFB 激光器开环校正步骤

Fig. 2　DFB laser open-loop correction steps

斜率的三角波驱动信号驱动 DFB 激光器，激光器出射激光经过自外差 MZI 后生成干涉信号；测试激光器的调频特性，当固定自外差 MZI 的参考臂光纤长度后，可以预测 DFB 激光器调频的理想拍频频率；光电探测器采集到拍频信号后，利用计算机分析拍频信号后得到时频信息；根据式(9)，利用拍频信号的时频信息与理想拍频频率可以得到激光器的非线性调谐量；确定激光器的非线性调谐量后，根据式(9)重塑三角波驱动信号，再次驱动激光器进行调频。

以上是基于迭代法的开环校正的方法，在实际的校正过程中，一次推导往往不能达到预期效果，采用多次迭代的方式可达到最终的要求。

2.3　闭环校正模型

建立了基于现场可编程门阵列(FPGA)的光电锁相环，其整体方案如图 3 所示。数/模转换器输出预制的三角波校正信号用于驱动 DFB 激光器模块，激光器输出的调频光经光隔离器进入分光比为 95∶5 的耦合器，95% 的光信号进入探测路，5% 的光信号进入校正路，光平衡探测器检测到自外差 MZI 输出的干涉信号中的拍频信号，经电压比较器输出晶体管-晶体管逻辑(TTL)电平的方波信号，方波信号中包含拍频信号的频率与相位信息，FPGA 中的鉴频鉴相器将此方波信号与参考信号的相位误差量化后输入自适应环路滤波器，自适应环路滤波器判断误差信号大小后将其量化加载到预制三角波信号中，建立闭环反馈系统。

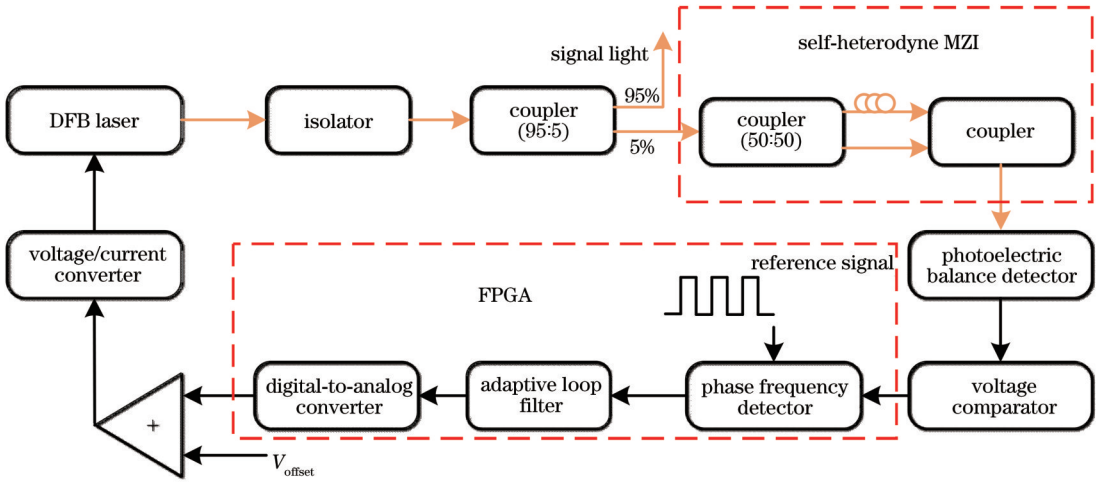

图 3　基于 FPGA 的光电锁相环系统整体方案

Fig. 3　Overall scheme of optoelectronic phase locked loop system based on FPGA

相较于传统的锁相环，文中的光电锁相环中 DFB 激光器模块至自外差 MZI 部分等效为压电振荡器，环路滤波器则由所设计的自适应环路滤波器替代。此处的环路滤波器与传统意义上的滤波器不同，其更重要的作用体现在对于相位误差信号的控制中，本文所采用的自适应环路滤波器基于比例积分(PI)控制的方式实现，其结构如图 4 所示。在对相位误差的量化过程中采用时间数字转换器(TDC)，TDC 方向控制器判断参考信号与方波信号的先后，相位误差量化的大小控制 PI 控制中的比例、积分参数，最终输出控制字并加载至预制三角波信号。本文构建的光电锁相环的 z 域等效模型如图 5 所示。图 5 中 θ_{erro} 为误差相位信息，θ_{ref} 为参考信号的相位，$\theta_{feedback}$ 为反馈信号的相位，f_{out} 为锁相环输出信号。

光电锁相环的闭环传递函数为

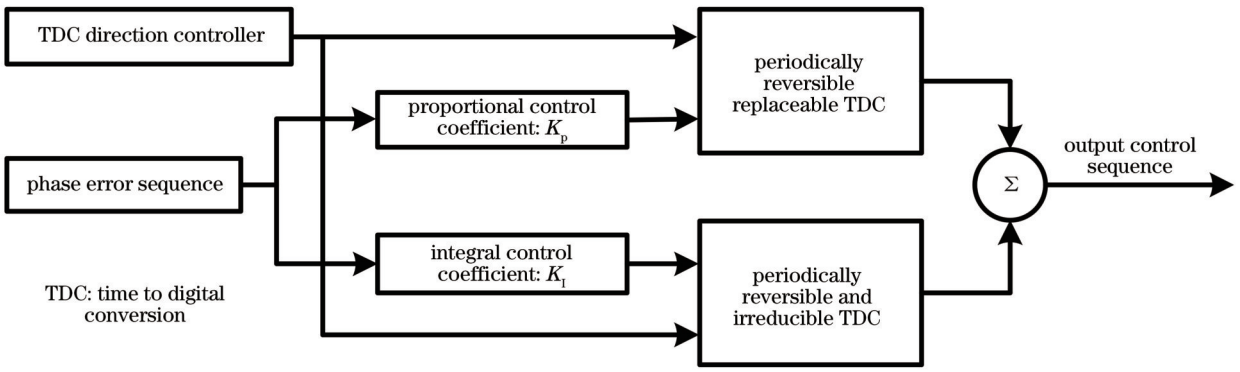

图 4　基于 PI 控制的自适应环路滤波器结构

Fig. 4　Adaptive loop filter structure based on PI control

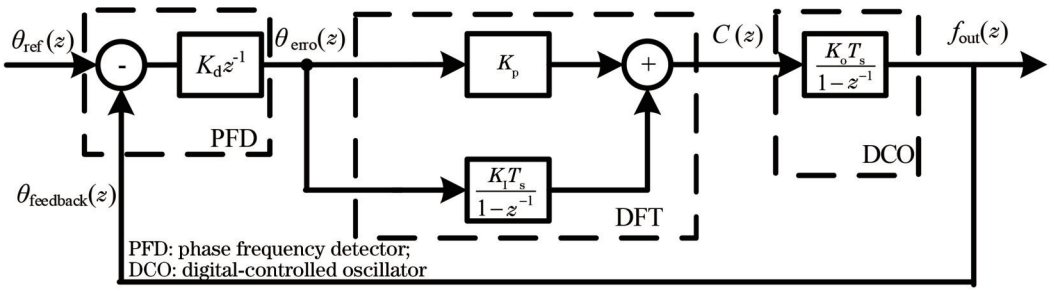

图 5　光电锁相环 z 域结构

Fig. 5　z-domain structure of optoelectronic phase-locked loop

$$H(z)=\frac{K_o K_d (K_P + K_I T_s) T_s z - K_o K_d K_P T_s}{z^2 + [K_o K_d (K_P + K_I T_s) T_s - 2] z + 1 - K_o K_d K_P T_s}, \tag{10}$$

式中：K_o 为 DCO 增益系数；K_d 为 PFD 增益系数；T_s 为系统采样间隔时间。

3　分析与讨论

本文采用绵阳全光通信科技有限公司的中心波长为 1550 nm 的 ECL-M-1550 分布反馈式半导体激光器，其输出光功率为 10 mW，线宽为 500 kHz，共模抑制比为 57 dB。利用信号发生器产生的 100 Hz 三角波信号驱动 DFB 激光器，利用光平衡探测器探测拍频信号，通过希尔伯特变换得到拍频信号的时间-频率曲线[图 6(a)]，对拍频信号进行 FFT，得到其 FFT 功率谱如图 6(b)所示，可以发现拍频信号的中心频率为 238.8 kHz，3 dB 带宽为 39.5376 kHz，功率为 −59.18 dBV。对于 DFB 激光器调频非线性的量化，往往分析拍频信号的时频曲线感兴趣区域的线性度，挑选时频曲线的部分信号作为判断标准，时频曲线的波动越小，则校正效果越好。本文对全周期拍频信号进行分析，通过拍频信号功率谱曲线中心频率的 3 dB 带宽来量化非线性。因此，原始三角波信号驱动下，DFB 激光器的非线性度为 16.55%。

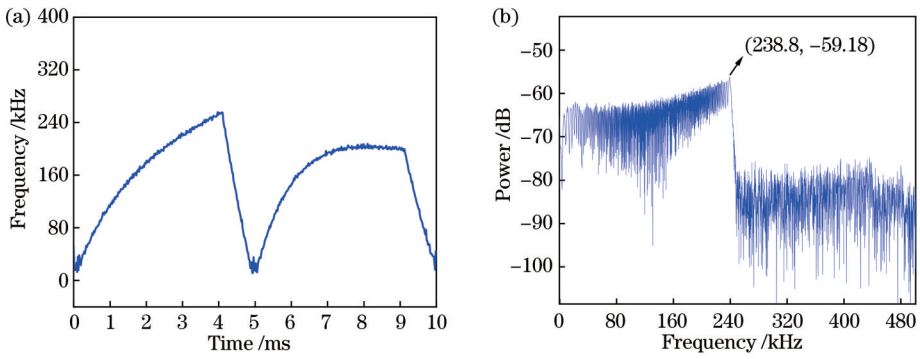

图 6　原始三角波信号驱动 DFB 激光器的结果。(a)拍频信号时频曲线；(b)拍频信号 FFT 功率谱

Fig. 6　Results of driving DFB laser with original triangular wave signal. (a) Time frequency curve of beat frequency signal; (b) FFT power spectrum of beat frequency signal

在开环校正实验中得到的迭代过程中拍频信号的时间-频率谱线如图 7 所示，可以发现第三次迭代的效果最优。在第三次迭代开环校正的结果中，拍频信号的中心频率为 174 kHz，3 dB 带宽减小为 6 kHz，功率为－48.22 dBV，光源的非线性度减小为 3.45%。

基于开环校正，引入本文所构建的光电锁相环，其中自外差 MZI 的臂长差设置为 5 m，如图 8(a)所示，由拍频信号的时间-频率曲线可以发现 80% 拍频信号被锁定在同一频率。如图 8(b)所示，拍频信号的中心频率为 169.4 kHz，3 dB 带宽减小至 132.169 Hz，非线性度减小至 0.078%，功率为－35.09 dBV，相较于未校正的 DFB 激光器，功率提高了 21.1 dB。

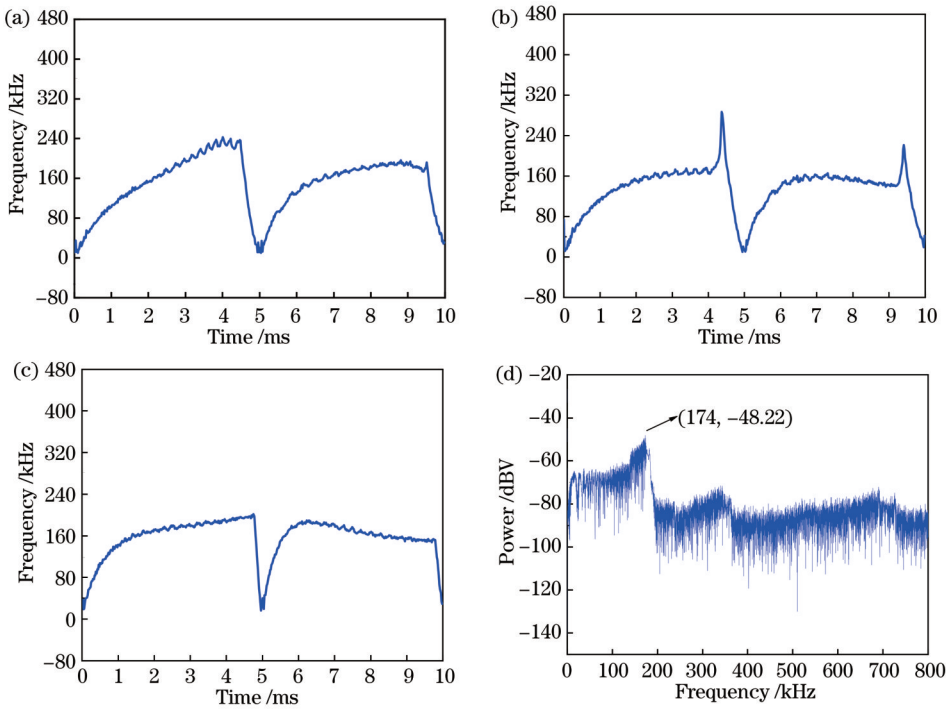

图 7　开环校正结果。(a)第一次迭代拍频信号时频曲线；(b)第二次迭代拍频信号时频曲线；(c)第三次迭代拍频信号时频曲线；(d)第三次迭代拍频信号 FFT 功率谱

Fig. 7　Open loop correction results. (a) Time-frequency curve of the first iteration beat frequency signal; (b) time-frequency curve of the second iteration beat frequency signal; (c) time-frequency curve of the third iteration beat frequency signal; (d) FFT power spectrum of the third iteration beat frequency signal

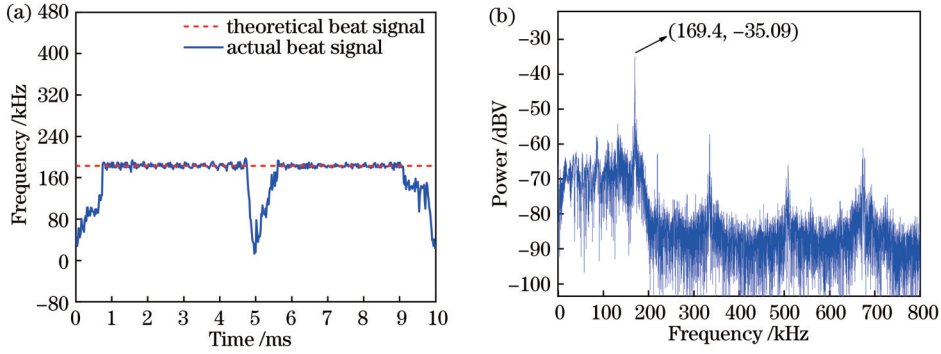

图 8　开环结合光电锁相环闭环校正结果。(a)拍频信号时频曲线；(b)拍频信号 FFT 功率谱

Fig. 8　Correction results of open loop combined with photoelectric phase-locked loop closed-loop. (a) Time frequency curve of beat frequency signal; (b) FFT power spectrum of beat frequency signal

为验证 DFB 激光器校正后的效果，设置待测光纤为 6 m，其拍频信号的 FFT 功率谱如图 9 所示，拍频信号中心频率的功率提高了 16.21 dB。

在此基础上，改变待测光纤长度，采用未校正光源对 3 m、6 m、12 m 与 15 m 的光纤进行测定，测量结果如表 1 所示，拟合曲线如图 10(a)所示，其拟合曲线的线性度为 0.99833。实验结果显示，在 0～15 m 范围内，系统测量值与真实值之间的最大误差为 0.3006 m，继续增加光纤长度，拍频信号的功率与噪声功率极其接近，信噪比低至无法分辨拍频信号。

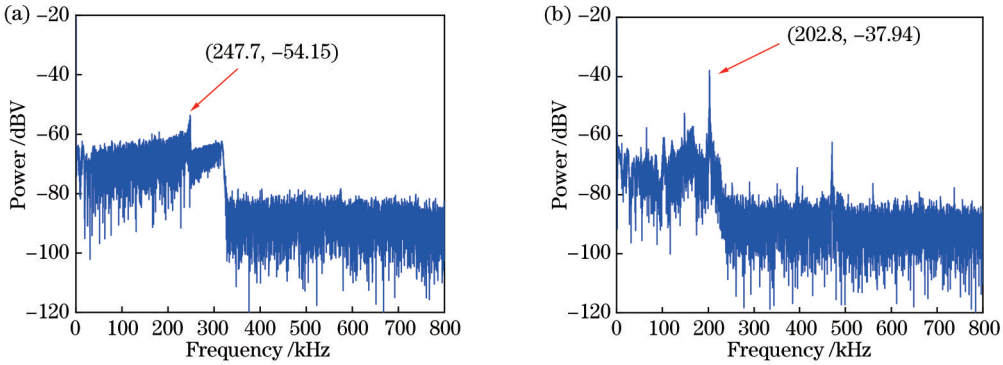

图 9　6 m待测光纤的拍频信号FFT功率谱。(a)采用未校正光源的测量结果;(b)采用校正后光源的测量结果

Fig. 9　FFT power spectra of beat frequency signal of 6 m fiber to be tested. (a) Measurement result using uncorrected light source; (b) measurement result using corrected light source

表 1　未校正光源的测量结果

Table 1　Measurement results using uncorrected light source

Length of FUT /m	Beat signal frequency /kHz	Fit measurement length /m	Error between measured value and true value /m
3	123.4	3.10333	0.10333
6	247.6	5.98104	−0.01896
12	494.4	11.69940	−0.30060
15	646.4	15.22120	0.22124

采用校正后光源对不同长度(3 m、12 m、21 m、39 m、48 m)光纤的测量数据进行标定,得到的拟合曲线如图 10(b)所示,拟合曲线的线性度为 1,之后对 6 m、33 m、36 m和 45 m光纤进行测定,其测量结果如表 2所示。实验结果显示,在 0~50 m范围内,系统的测量值与真实值之间的最大误差为 0.00379 m,即 3.79 mm。

为了进一步验证对DFB激光器的校正效果,本文

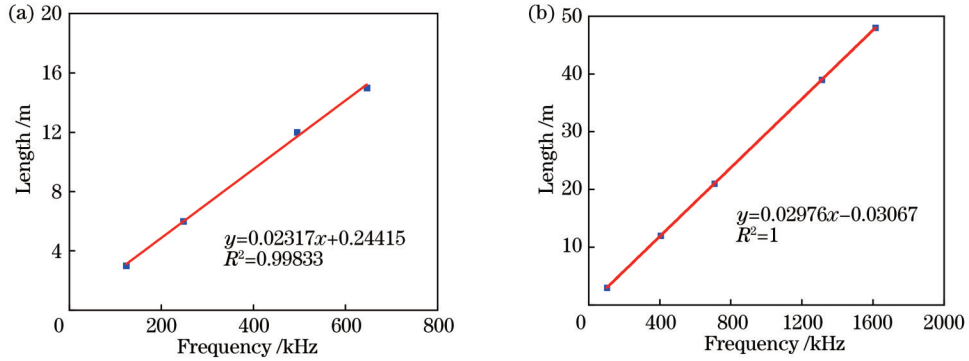

图 10　对光纤测量结果的拟合曲线。(a)采用未校正光源对光纤测量结果的拟合曲线;(b)采用校正光源对光纤测量结果的拟合曲线

Fig. 10　Fitting curves for fiber measurement results. (a) Fitting curve of fiber measurement results for uncorrected source; (b) fitting curve of fiber measurement results for corrected source

表 2　校正后光源的测量结果

Table 2　Measurement results of corrected light source

Length of FUT /m	Beat signal frequency /kHz	Fit measurement length /m	Error between measured value and true value /m
6	202.600	5.99870	−0.00130
33	1110.000	33.00293	0.00293
36	1210.800	36.00270	0.00270
45	1513.000	44.99621	−0.00379

对待测光纤进行重复性测量，待测光纤重复性测量结果如图 11 所示，其中 20 次重复测量的误差曲线如图 11(a)所示，不同长度待测光纤的误差棒曲线如图 11(b)所示，分析得到系统在 45 m 处的重复性测量误差最大，其标准偏差为 112.2 μm。

本文最终实验的最大探测距离为 50 m，这并不代表基于电流直接调制 DFB 激光器的 OFDR 技术探测极限，与最大探测距离密切相关的重要指标是光源的调频非线性与光源的线宽。本文实验验证了随着光源调频非线性的降低，系统的最大探测距离增加，光源的线宽则直接影响其相干长度。本文所采用的 500 kHz 线宽激光器的相干长度为 600 m，因此调频非线性的进一步降低有助于进一步增大系统的最大探测距离，通过更精确的开环校正方法与线宽更窄、功率更高的 DFB 激光器，可提升 OFDR 系统的分辨率并增大探测距离。

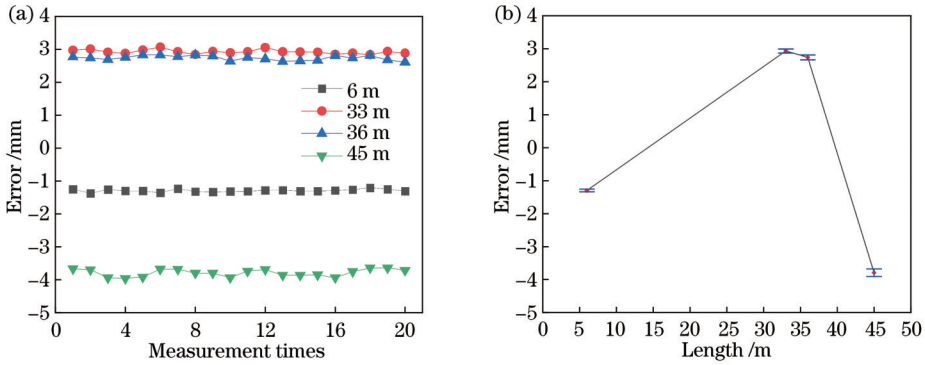

图 11 待测光纤重复性测量结果。(a) 20 次重复测量误差曲线；(b) 不同长度待测光纤的误差棒曲线

Fig. 11 Reproducibility measurement results of FUT. (a) Error curves of 20 repeated measurements; (b) error bar curve of FUT with different lengths

4 结 论

针对 OFDR 系统中的电流直接调制 DFB 激光器光源调频的非线性问题，提出了开环校正结合光电锁相环闭环校正 DFB 激光器的方法，从而提高 OFDR 系统的分辨率。实验验证了校正后的光源非线性度下降至 0.078%，拍频信号的中心频率处的功率相较于未校正时提高了 21.1 dB，在 50 m 的探测范围内实现了 3.79 mm 的最大误差，系统重复性测量的最大标准偏差为 112.2 μm。未来可通过采用更精确的开环校正方法或借助线宽更窄、功率更高的 DFB 激光器等方式，进一步提升 OFDR 系统的分辨率、增大探测距离。

参 考 文 献

[1] Qu S, Xu Y P, Huang S, et al. Recent advancements in optical frequency-domain reflectometry: a review[J]. IEEE Sensors Journal, 2023, 23(3): 1707-1723.

[2] Zhang C, Bao Y, Cui T, et al. Polarization independent phase-OFDR in Rayleigh-based distributed sensing[J]. Journal of Lightwave Technology, 2023, 41(8): 2518-2525.

[3] Liu S Q, Yu F H, Hong R, et al. Advances in phase-sensitive optical time-domain reflectometry[J]. Opto-Electronic Advances, 2022, 5(3): 200078.

[4] Lu L D, Su X C, Zhang C L, et al. A novel distributed vibration sensor based on fading noise reduction in multi-mode fiber[J]. Sensors, 2022, 22(20): 8028.

[5] Yuan H Y, Wang Y, Zhao R, et al. An anti-noise composite optical fiber vibration sensing system[J]. Optics and Lasers in Engineering, 2021, 139: 106483.

[6] Lu L D, Yong M C, Wang Q S, et al. A hybrid distributed optical fiber vibration and temperature sensor based on optical Rayleigh and Raman scattering[J]. Optics Communications, 2023, 529: 129096.

[7] Ba D X, Qiu L Q, Chu Q, et al. High-resolution and large-strain distributed dynamic sensor based on Brillouin and Rayleigh scattering[J]. Optics Letters, 2022, 47(22): 5777-5780.

[8] Sladen A, Rivet D, Ampuero J P, et al. Distributed sensing of earthquakes and ocean-solid Earth interactions on seafloor telecom cables[J]. Nature Communications, 2019, 10: 5777.

[9] Qin Z J, Hu Y W, Yue Y L, et al. A dual-ended 400 km OFDR for vibration detection[J]. Measurement Science and Technology, 2022, 33(4): 045203.

[10] 刘琨，冯博文，刘铁根，等. 基于光频域反射技术的光纤连续分布式定位应变传感[J]. 中国激光，2015，42(5)：0505006.
Liu K, Feng B W, Liu T G, et al. Continuous distributed fiber strain location sensing based on optical frequency domain reflectometry[J]. Chinese Journal of Lasers, 2015, 42(5): 0505006.

[11] Xu B J, He J, Du B, et al. Femtosecond laser point-by-point inscription of an ultra-weak fiber Bragg grating array for distributed high-temperature sensing[J]. Optics Express, 2021, 29(20): 32615-32626.

[12] 陈典，莫文静，赵正大，等. 基于光频域反射仪的机载光缆连接检测技术[J]. 测控技术，2022，41(10)：119-123.
Chen D, Mo W J, Zhao Z D, et al. Airborne optical cable connection detection technology based on optical frequency domain reflectometer[J]. Measurement & Control Technology, 2022, 41(10): 119-123.

[13] Okamoto T, Iida D, Koshikiya Y, et al. Deployment condition visualization of aerial optical fiber cable by distributed vibration sensing based on optical frequency domain reflectometry[J]. Journal of Lightwave Technology, 2021, 39(21): 6942-6951.

[14] Mustafa S, Sekiya H, Morichika S, et al. Monitoring internal strains in asphalt pavements under static loads using embedded distributed optical fibers[J]. Optical Fiber Technology, 2022, 68: 102829.

[15] Fernández M P, Morbidel L, Bulus-Rossini L A, et al. Temperature-robust monitoring of TDM-PONs through optical coding assisted by broadband λ-tunable I-OFDR[J]. Journal of

Lightwave Technology, 2021, 39(14): 4607-4613.
[16] Wang J Q, Li Z Y, Yang Q, et al. Interrogation of a large-capacity densely spaced fiber Bragg grating array using chaos-based incoherent-optical frequency domain reflectometry[J]. Optics Letters, 2019, 44(21): 5202-5205.
[17] Esquivel-Hernández J, Martínez-Manuel R. Resolution improvement in a multi-point fiber refractometer based on coherent-OFDR[J]. IEEE Photonics Technology Letters, 2020, 32(9): 530-533.

High Spatial Resolution OFDR Based on In-Current Modulation of DFB Laser

Zhang Jiatong, Su Liwen, Liu Chang, Chu Yanyan, Fu Xinghu, Jin Wa, Bi Weihong, Fu Guangwei*

Key Laboratory for Special Fiber and Fiber Sensor of Hebei Province, School of Information Science and Engineering, Yanshan University, Qinhuangdao 066004, *Hebei, China*

Abstract

Objective Optical frequency domain reflectometry (OFDR) systems feature high precision, high resolution, large range, strong real-time performance, and high signal-to-noise ratio. Therefore, OFDR technology has broad application prospects in aviation, transportation, and communication. After decades of this technological development, the bottleneck for its further development is that it is difficult to realize the sweep light source and optimize the signal processing, and the performance, precision, and resolution of the system are directly affected by the frequency-modulated linearity of the light source. At present, the light source employed in the system is a mechanically tuned diode laser with a wide frequency-modulated range and a narrow linewidth, but it is difficult to reduce the cost and extend the service life. The direct current modulation of distributed feedback semiconductor (DFB) lasers is a potential high-quality light source for OFDR systems because of its low cost and simple frequency modulation, but the phase noise and poor linearity of frequency modulation must be solved. Thus, we discuss the frequency modulation nonlinearity of light source in the OFDR system, such as the location difference of the sensor unit, low sensor precision, narrow sensor range of the sensor, and poor system adaptability, and propose an open-loop correction method combined with an optoelectronic phase-locked loop closed-loop correction for DFB laser.

Methods The method of open-loop correction combined with photoelectric phase-locked loop closed-loop correction for DFB lasers is adopted to control the continuous, fast, and large-range frequency scanning linearization of DFB lasers. As a result, it becomes a high-quality light source for the OFDR system and improves the OFDR resolution. First, based on the direct current modulation characteristics of DFB lasers and the idea of iterative open-loop correction, the DFB laser is initially corrected, and the correction effect is evaluated by the time-frequency curve of the beat signal and the FFT power spectrum curve. Then, the closed-loop correction method is introduced, and the closed-loop correction is realized by constructing the corresponding oscillator, loop filter, and phase discriminator structure in the photoelectric phase-locked loop. The correction results are evaluated, and the fixed fiber length is measured for the sweep frequency nonlinearity correction system and the uncorrected DFB laser to show the correction effect.

Results and Discussions For the uncorrected DFB laser, the beat signal center frequency is 238.8 kHz, the 3 dB bandwidth is 39.5376 kHz, the power is −59.18 dBV, and the nonlinearity of the light source is 16.55% (Fig. 6). After the open-loop correction, the sweep nonlinearity of the DFB laser is reduced to 174 kHz, the bandwidth of 3 dB is reduced to 6 kHz, the power is −48.22 dBV, and the light source nonlinearity is reduced to 3.45% (Fig. 7). Meanwhile, the central frequency of the beat frequency signal is 169.4 kHz, the 3 dB bandwidth is reduced to 132.169 Hz, and the nonlinearity is reduced to 0.078% after the closed-loop correction of the photoelectric phase-locked loop, with the power of −35.09 dBV (Fig. 8). The proposed method has a good correction effect on the sweep nonlinearity of DFB lasers. Additionally, in the experiment of measuring the optical fiber length, the maximum error between the measured and true values of the system is 0.3006 m in the range of 0–15 m for the uncorrected light source (Table 1), which continues to increase the optical fiber length. The beat signal power is very close to the noise power, and the low signal-to-noise ratio makes the beat signal cannot be distinguished. The maximum error between the measured and true values is 3.79 mm (Table 2). The system shows a longer measuring range and a smaller error, and the corrected system exhibits stronger

stability with a maximum standard deviation of 112.2 μm for repeatability system measurements over a 50 m probe range (Fig. 11).

Conclusions We put forward the method of open-loop correction combined with photoelectric phase-locked loop correction for DFB lasers to solve the frequency modulation nonlinearity of DFB laser source in the OFDR system, thus improving the resolution of OFDR systems. The experiment shows that the nonlinearity of the corrected light source is reduced to 0.078%, and the central frequency power of the beat frequency signal is increased by 21.1 dB compared with the uncorrected one. The maximum error of 3.79 mm is achieved in the detection range of 50 m and the maximum standard deviation of repeatability measurements is 112.2 μm. The maximum detection distance of 50 m in the final experiment does not represent the detection limit of OFDR technology based on direct current modulation of DFB lasers. The important indexes closely related to the maximum detection distance are the frequency modulation nonlinearity and the light source linewidth. The experiment proves that the maximum detection distance of the system increases with the reduced frequency modulation nonlinearity of the light source, and the light source linewidth directly affects its coherence length. Therefore, the further reduction of frequency modulation nonlinearity helps further increase the maximum detection distance of the system by a more accurate open-loop correction method with narrower linewidth and higher-power DFB lasers, improving the resolution and detection distance of the OFDR system. In the future, the resolution and detection distance of the OFDR system can be further improved by a more accurate open-loop correction method or DFB lasers with narrower linewidth and higher power.

Key words lasers; distributed feedback semiconductor lasers; optical frequency domain reflection; frequency scanning linearization; photoelectric phase-locked loop